BIOCHEMISTRY
including biophysical chemistry & molecular biology

Article

pubs.acs.org/biochemistry

Role of Arginine 29 and Glutamic Acid 81 Interactions in the Conformational Stability of Human Chloride Intracellular Channel 1

Derryn Legg-E'Silva,[†] Ikechukwu Achilonu,[†] Sylvia Fanucchi,[†] Stoyan Stoychev,[†] Manuel Fernandes,[‡] and Heini W. Dirr*[,†]

[†]Protein Structure−Function Research Unit, School of Molecular and Cell Biology, University of the Witwatersrand, Johannesburg 2050, South Africa

[‡]School of Chemistry, University of the Witwatersrand, Johannesburg 2050, South Africa

Supporting Information

ABSTRACT: The ion channel protein CLIC1 exists in both a soluble conformation in the cytoplasm and a membrane-bound conformation. The conformational stability of soluble CLIC1 demonstrates pH sensitivity which may be attributable to very specific residues that function as pH sensors. These sensors could be histidine or glutamate residues with pK_a values that fall within the physiological pH range. The role of Glu81, a member of a topologically conserved buried salt bridge in CLIC1, as a pH sensor was investigated here. The mutants E81M, R29M, and E81M/R29M were designed to break the salt bridge between Glu81 and Arg29 and examine the effect of each member on the stability of the protein. Spectroscopic studies and the solved crystal structures indicated that the global structure of CLIC1 was not affected by the mutations. Urea-induced equilibrium unfolding unexpectedly showed E81M to stabilize CLIC1 at pH 7. This was due to stabilizing hydrophobic interactions with Met81 and a water-mediated compensatory H-bond between Met81 and Arg29. R29M and E81M/R29M destabilized CLIC1 at pH 7, and the unfolding transition changed from two-state to three-state, mimicking the wild type at pH 5.5. This observation points out the significance of the salt bridge in stabilizing the native state. The total unfolding free energy change of E81M CLIC1 does not change with pH, implying that Glu81 forms one of a network of pH-sensor residues in CLIC1 responsible for destabilization of the native state. This allows detachment of the N-domain from the C-domain at low pH.

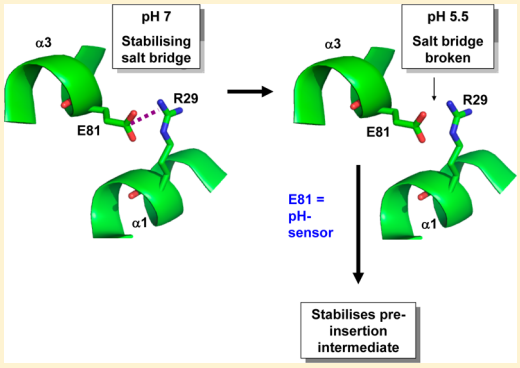

Chloride intracellular channels (CLICs) occur on the plasma membrane of most eukaryotic cells as well as in other intracellular membranes[1,2] and are implicated in several physiological processes.[3] The CLIC protein family consists of seven members, namely, CLICs 1−5A, CLIC5B, and CLIC6,[4,5] that show high sequence identity of between 47% and 76%.[1] CLIC proteins exist in both a soluble and a membrane-bound form (reviewed in refs 1, 6, and 7). The mechanism of conversion between these conformations is unknown, although pH[8,9] and oxidation[4] have been proposed to be involved. Furthermore, CLIC1 has been categorized as a metamorphic or fold-switching protein as it has been shown to adopt different native folds, whether in an oxidized or reduced state.[4]

Soluble reduced human CLIC1 is monomeric and consists of an N-domain with a thioredoxin-like fold and an all α-helical C-domain. Helices α1 and α3 from the N-domain form the domain interface of CLIC1, and most of the interdomain interactions are provided by helix α1. It is helix α1 and strand β2 from the N-domain that are believed to form the transmembrane region.[2,6,10−12] Furthermore, the N-domain is more flexible than the C-domain.[9] Therefore, the N-domain has the intrinsic propensity to alter its fold in order to prime the protein for membrane insertion. Since the stability of CLIC1 has been shown to be pH dependent and an equilibrium intermediate species that could resemble a preinsertion state has been detected at low pH,[8] we question whether changes in the ionization states of residues within the flexible regions of the N-domain in response to pH changes could alter the stability of the soluble state of the protein. These residues could then be described as being pH sensors crucial to pH-induced structural changes that occur when the soluble protein approaches the low-pH environment at the membrane surface[13,14] prior to membrane insertion. Particularly, we addressed the idea that salt bridges may be involved in the pH-induced conformational stability changes of soluble CLIC1.[15−19]

A topologically conserved hydrogen bond and salt bridge interaction between the N- and C-domains across the CLIC family was identified between Arg29 and Glu81 (Figure 1). The intrinsic pK_a values of the ionizable groups of Arg29 and Glu81 could change depending on a number of factors such as the degree of solvent exposure, the presence of formal charges, and

Received: June 29, 2012
Revised: September 11, 2012
Published: September 11, 2012

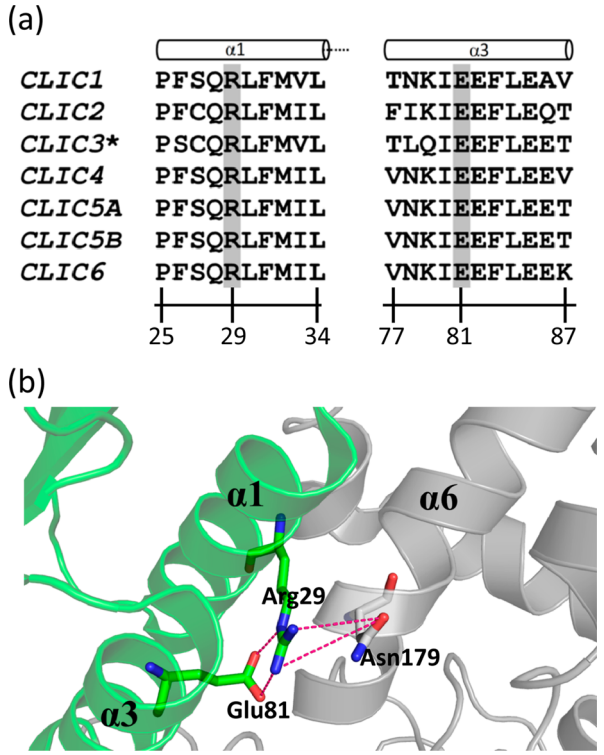

Figure 1. Structural and sequence information on CLIC. (a) Summarized figure on the structural alignment of mammalian and invertebrate CLIC family (cylinders represent helices and broken line represents truncated secondary structure). Residues in a corresponding position to the human CLIC1 Arg29 and Glu81 residues are highlighted. CLIC sequences were retrieved from the UniProtKB database, and the alignment was performed with the 3DCoffee[54] Web-interface program. The database accession number for the sequences used for the alignment are O00299 (CLIC1), O15247 (CLIC2), Q9D7P7 (mouse CLIC3*), Q9Y696 (CLIC4), Q9Y696 (CLIC5A), Q9NZA1 (CLIC5B), and Q96NY7 (CLIC6).The numbering is based on human CLIC1. (b) Ribbon representation of wild-type human CLIC1 (PDB ID: 1K0M) showing H-bond interaction mediated by Arg29, Glu81, and Asn179 that contributes to the packing of helix1, helix3, and helix6 at the N-domain (green) and C-domain (gray). The figure was produced with PyMol.[36]

the degree of burial or exposure of the group. Furthermore, when hydrogen bonds are made with ionizable groups, the hydrogen bonds can increase or decrease the pK_a by several pH units.[20]

In this study, we systematically replaced Arg29 and/or Glu81 with methionine to form R29M, E81M, and R29M/E81M mutants. These mutations were designed to break the salt bridge H-bond interaction between Arg29 and Glu81 as well as other hydrogen bonds connecting them together. The mutations were also hypothesized to alter the hydrogen-bonding interactions with Asn78 on helix α3 and Asn179 on helix α6 and thereby alter the packing of the protein at the domain interface. The rationale behind creating these mutants was that the side chain of methionine will maintain bulk but alter charge and allow us to assess the effect of the buried salt bridge and particularly the negative charge on Glu81 on the stability of the soluble conformation of CLIC1.

MATERIALS AND METHODS

Site-Directed Mutagenesis, Protein Expression, and Purification. The ORF of human CLIC1 was extracted from the GenBank database (ID: AF034607.1), and the nucleotide sequence encoding the human CLIC1 was used to construct the following mutagenic primers: 5′cacagacaccaacaagattatggaatttctggaggcagtgc3′ (for E81M-CLIC1) and 5′ctgcccattctccagatgctgttcatggtactgtgg-3′ (for R29M-CLIC1). The mutant codons are underlined. The primers and their corresponding reverse complements were synthesized at Inqaba Biotec (Pretoria, South Africa). Recombinant pGEX-4T-1 encoding wild-type CLIC1 ORF (a gift from S. N. Breit, Centre for Immunology, St. Vincent's Hospital, and University of New South Wales, Sydney Australia) was used as a template for the site-directed mutagenesis reactions using the QuickChange site-directed mutagenesis kit (Stratagene, La Jolla, CA) according to the manufacturer's instruction. The plasmids were sequenced to confirm the presence of the mutation at Inqaba Biotec (Pretoria, South Africa). The mutant plasmids were used to transform *Escherichia coli* BL21 (DE3) pLysS strains for overexpression and purification of the proteins as previously described for wild type[8] with the only exception being that induction of E81M CLIC1 expression was done at 20 °C rather than at 37 °C. Size exclusion chromatography (Sephadex G-75, 50 cm × 3.2 cm) was used to obtain additional purity required for crystallography. Protein purity was confirmed by SDS-PAGE on a 12.5% acrylamide gel according to the method of Laemmli.[21]

Spectroscopic Studies. The degree of exposure (K_{sv}) of the lone Trp35 residue as a result of the mutation was determined by acrylamide quenching studies.[22] Briefly, acrylamide (0−0.3 M) was added to 2 μM protein (in 50 mM Na_2HPO_4, 1 mM DTT, 0.02% (w/v) NaN_3) after which Trp35 was selectively excited at 295 nm, and the fluorescence maximum was monitored at 345 nm using a PerkinElmer LS-50B luminescence spectrometer. The data were plotted using SigmaPlot v11.0 and analyzed according to the conventional Stern−Volmer equation:

$$F_0/F = 1 + K_{sv}[Q]$$

where F_0 and F are the fluorescence intensities in the absence and presence of quencher, respectively. K_{sv} is the Stern−Volmer constant for collisional quencher processes, and [Q] is the concentration of acrylamide.

For urea-induced equilibrium unfolding, 2 μM protein at pH 5.5 or 7.0 was left to equilibrate in 0−8 M urea at 20 °C. The global structure was monitored by far-UV CD at 222 nm. Changes within the local environment were monitored using fluorescence by excitation at 280 nm and by ANS-binding using an excitation wavelength of 350 nm and an emission wavelength of 470 nm as previously described.[8] The reversibility of CLIC1 denaturation under these conditions was previously confirmed for the wild type[8] as well as the mutants. Five different probes were used to monitor the global unfolding: (i) ellipticity at 222 nm to monitor the secondary structure, (ii) fluorescence at 345 nm, (iii) fluorescence at 310 nm, (iv) fluorescence at 320 nm, and (v) fluorescence at 330 nm to monitor the tertiary structure. The data from equilibrium unfolding experiments were globally fit to either a two-state monomer (N ↔ U) model or a three-state monomer (N ↔ I ↔ U) model using Savuka version 6.2.26.[23,24] The thermodynamic parameters, $\Delta G^\circ_{H_2O}$ (kcal mol^{-1}) and m values (kcal mol^{-1} M^{-1}), obtained from the global fits using the linear extrapolation method were used to calculate the fractional population of each species from the equilibrium constants.[25]

dx.doi.org/10.1021/bi300874b | *Biochemistry* 2012, 51, 7854−7862

Protein Crystallization, X-ray Diffraction, and Structure Solution. The optimum conditions for crystallization of E81M CLIC1 and R29M/E81M CLIC1 were predetermined using the Hampton Index HR2-144 solutions for crystal growth at pH 5.5, 6.5, and 7.0 (Hampton Research, Aliso Viejo, CA). Briefly, crystals were grown by the hanging drop vapor diffusion method at 293 K using a 24-well greased VDX plate (Hampton Research, Aliso Viejo, CA). E81M crystals were grown in reservoir buffer comprising 0.1 M Bis-tris, pH 6.5, 0.2 M ammonium acetate, 30% (w/v) PEG 3350 (0.5 1.0 mL per well), and R29M/E81M crystals were grown in reservoir buffer comprising 0.1 M Bis-tris, pH 6.5, 20% (v/v) PEG 2000 (0.5−1.0 mL per well). Each hanging drop (2, 6, and 8 μL) was made by mixing equal volume of stock protein solution [10 mg mL^{-1} in 0.1 M Tris-HCl, pH 6.5, 5 mM DTT and 0.02% (w/v) NaN_3] with the reservoir buffer. The crystals were harvested, soaked in a cryo-protectant [25% (v/v) glycerol in the mother liquor], mounted on a cryo-loop, and snap-frozen in liquid nitrogen. X-ray diffraction data were collected on a Bruker X8 PROTEUM X-ray diffractometer equipped with a Microstar copper rotating anode generator, Montel Optics, a PLATINUM 135 CCD detector, and an Oxford CryoStream Plus system. Crystals were cooled to 113 K in a stream of nitrogen during data collection, and images were collected covering an oscillation angle of 0.5° per frame. The data sets were indexed with APEX and SAINT software.[26] The structures were solved by molecular replacement using PHASER[27,28] implemented in the CCP4i suite of programmes.[29] The molecular replacement search model structure for both set of crystals was 3O3T (PDB ID).[30] The models were refined with REFMAC5,[31] and model building was performed with Coot.[32] Solvent molecules were added to the models after several rounds of refinement. Stereochemical validation of the models was performed using ProCheck[33] and MolProbity.[34] The data collection and refinement statistics are given in Table 1. SPDBV v 4.0[35] was used to align two or more structures and compute H-bonding. PyMol[36] was used to generate images of the structures.

RESULTS

The main objective of this study was to identify and characterize residues and/or interactions in the N-domain that stabilize the structure and stability of the soluble form of CLIC1. This study was performed as a function of pH in order to gain a better understanding of how the conformational stability of soluble (cytosolic) CLIC1 at pH 7 changes when it is exposed to the acidic (pH 5.5) environment at the surface of the membrane. This study is not concerned with membrane insertion; it is based on the current understanding that soluble CLIC1 undergoes a degree of unfolding/restructuring prior to membrane insertion.[2] The significance of this study is that it assesses the changes to soluble CLIC1 when it encounters reduced pH near the membrane and the role of pH sensors in these changes.

Structural Integrity of the CLIC1 Mutant Proteins. The wild-type CLIC1 and mutant proteins displayed similar far-UV CD and fluorescence spectra that indicated that the mutations did not cause significant global changes to the CLIC1 protein (Figures S1 and S2). This was confirmed by the crystal structures of the E81M and R29M/E81M mutants. The ability of acrylamide to quench tryptophan fluorescence is a useful way of determining the exposure of tryptophan to the solvent.[22] The K_{sv} values (Table 2) for quenching of the wild-type CLIC1 and mutant proteins were relatively high, which is consistent with a protein with a partially exposed tryptophan residue.[22] The K_{sv} values were similar to each other at both experimental pH values. Also, the values for the CLIC1 mutant proteins were similar to wild-type CLIC1 at both experimental pH values (Table 2). The acrylamide quenching thus shows that the mutations do not appear to significantly alter the exposure of the Trp35 residue to the solvent (Figure S3). The conclusion from all the above spectroscopic studies on the structural integrity of CLIC1 is that the mutations do not result in significant modifications of the native structure of CLIC1.

Table 1. Crystallographic X-ray Data Collection and Refinement Statistics for Human CLIC1 Mutants R29M/E81M and E81M[a]

	R29M/E81M	E81M
PDB code	3P8W	3UVH
	Data Collection via CCD	
wavelength (Å)	1.5418	1.5418
space group	$P2_12_12_1$	$P2_1$
unit cell dimensions (Å)	a = 42.4	a = 42.5
	b = 83.0	b = 70.1
	c = 64.6	c = 82.7
	$\alpha = \beta = \gamma = 90°$	$\alpha = \beta = \gamma = 90°$
resolution (Å)	51.0−1.79 (1.79−1.89)	82.7−1.84 (1.84−1.91)
R_{sym} (%)	27.7 (61.9)	34.3 (73.2)
$I/\sigma(I)$	12.4 (3.97)	12.8 (2.04)
completeness (%)	99.1 (95.2)	99.6 (97.1)
no. of reflections	164224	269700
no. of unique reflections	21873 (2996)	41890 (5299)
Matthews coeff ($Å^3$)	2.11	2.28
solvent content (%)	41.7	46.1
	Refinement	
resolution (Å)	51.0−2.0 (2.00−2.05)	37.7−1.84 (1.84−1.89)
R_{cryst}/R_{free}	0.21/0.28	0.20/0.26
no. of reflections	15972 (1116)	41848 (2714)
B-factor ($Å^2$)	16.3	22.3
completeness (%)	99.8 (100)	99.7 (95.7)
no. of protein atoms	1850	3642
solvent molecules	188	439
rmsd bond lengths (Å)	0.019	0.018
rmsd bond angles (deg)	1.758	1.861
	Ramachandran Analysis (%)	
favored	97.9	97.2
allowed	1.7	2.1
disallowed	0.4	0.7

[a]All values in parentheses are for the highest-resolution shell.

Table 2. K_{sv} and Fit Statistics Values for the Quenching of Fluorescence by Acrylamide

	pH 7		pH 5.5	
CLIC1	K_{sv}	R^2	K_{sv}	R^2
wild type	9.5 ± 0.3	0.98	8.2 ± 0.1	0.99
R29M	10.2 ± 0.3	0.97	10.4 ± 0.4	0.96
E81M	10.5 ± 0.3	0.98	11.1 ± 0.5	0.95
R29M/E81M	9.6 ± 0.3	0.96	10.1 ± 0.3	0.98

dx.doi.org/10.1021/bi300874b | Biochemistry 2012, 51, 7854−7862

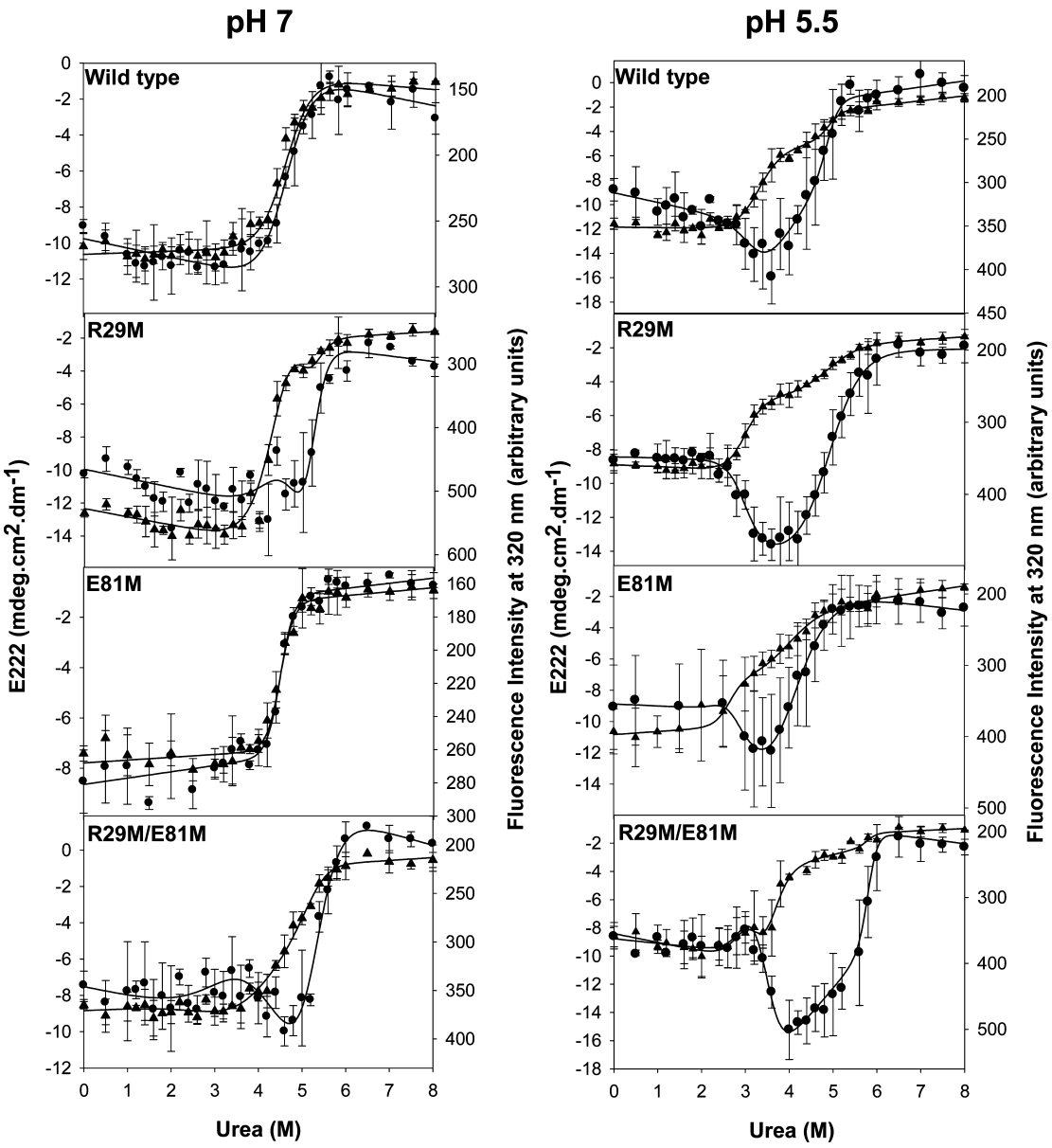

Figure 2. Equilibrium unfolding of CLIC1 wild-type and mutant at pH 7 and pH 5.5 as monitored by ellipticity at 222 nm (●) and fluorescence intensity at 345 nm (▲). The lines represent the best global fits of the two-state and three-state models to the data. Experiments were conducted at 20 °C with 2 μM CLIC1.

Conformational Stability of the Wild-Type and Mutant CLIC1. In order to assess the effect of the mutations on the conformational stability of CLIC1, urea-induced equilibrium unfolding studies were performed on the proteins and the results compared to the wild type at both pH 7 and pH 5.5. The unfolding of the mutants was reversible at both pH values as is the case with the wild type.[8] It is evident that the unfolding curves of wild-type CLIC1 and E81M at equilibrium at pH 7 are single sigmoidal curves. The far-UV CD and fluorescence data superimpose throughout the transition, and the slopes of the curves show that the loss of secondary structure and the tertiary environment of Trp35 occur simultaneously. However, the unfolding data monitored by far UV-CD and fluorescence spectroscopy for R29M and R29M/E81M at pH 7 are not superimposable (Figure 2). The two individual data sets for R29M and R29M/E81M separate within the transition region between 3 and 6 M urea, suggesting the presence of intermediate species along the equilibrium unfolding transition.

The far-UV CD and fluorescence unfolding data of all the individual proteins when monitored at pH 5.5 are not single sigmoidals (Figure 2). The transition regions are broader and shifted to lower urea concentrations compared to the transition regions of the unfolding data at pH 7. The slopes of the transition curves at pH 5.5 show that the loss of secondary structure and changes in the local environment of Trp35 have reduced cooperativity when compared to pH 7 (Figure 2). The results obtained for the urea-induced equilibrium unfolding at pH 5.5, therefore, indicate that significant populations of intermediate species accumulate at pH 5.5 at equilibrium under mild denaturing conditions.[37]

Since the pH 7 data for wild-type CLIC1 and E81M are monophasic, the intrinsic fluorescence intensities at various wavelengths as well as the ellipticity at 222 nm (E222) were

dx.doi.org/10.1021/bi300874b | *Biochemistry* 2012, 51, 7854−7862

globally fit to a two-state monomer model (N ↔ U)[23] (Figure S4). The thermodynamic parameters ΔG°_{nu} and m_{nu} generated by the global fitting of the E81M mutants' unfolding data at pH 7 were increased relative to those of wild-type CLIC1 (Table 3). This indicates that the E81M mutation appears to have caused an increase in the conformational stability as well as the cooperativity of CLIC1 unfolding. The R29M and R29M/E81M mutants seem to mimic the behavior of wild-type CLIC1 at pH 5.5 when at pH 7 in that they unfold via a three-state transition with a highly populated and energetically favorable intermediate species present under mild denaturing conditions. The impact of these mutations on the CLIC1 protein at pH 7 is a loss in the cooperativity of unfolding of the proteins.

Table 3. ΔG° (kcal mol^{-1}) and *m*-Values (kcal mol^{-1} M^{-1}, in Parentheses) of Wild-Type and Mutant CLIC1 Determined from Global-Fitted Far-UV CD and Fluorescence Curves

	equilibrium transition 1		equilibrium transition 2	
protein	pH 7.0	pH 5.5	pH 7.0	pH 5.5
wild type[a]	9.2 ± 0.7	7.5 ± 2.2		18.8 ± 5.5
	(2.0 ± 0.1)	(2.3 ± 0.7)		(3.8 ± 1.1)
R29M	9.1 ± 1.5	8.3 ± 1.4	19.6 ± 3.6	7.8 ± 0.7
	(2.0 ± 0.4)	(2.8 ± 0.5)	(3.7 ± 0.7)	(1.6 ± 0.1)
E81M[a]	16.8 ± 1.5	8.9 ± 4.9		5.8 ± 0.5
	(3.7 ± 0.3)	(3.3 ± 1.9)		(1.5 ± 0.1)
R29M/E81M	4.3 ± 1.6	7.0 ± 1.9	11.6 ± 1.6	3.2 ± 2.1
	(1.2 ± 0.5)	(1.8 ± 0.6)	(2.2 ± 0.3)	(0.7 ± 0.3)

[a]Monophasic (two-state) equilibrium transition at pH 7.0.

The $\Delta G^{\circ}_{H_2O}$ and *m* values of the R29M, E81M, and R29M/E81M mutants for the N ↔ I transition are similar to those of wild-type CLIC1 at pH 5.5 (Table 3). However, lower $\Delta G^{\circ}_{H_2O}$ and *m* values for the I ↔ U transitions for the R29M, E81M, and R29M/E81M mutants indicate that their intermediate species at pH 5.5 are energetically less stable than that of the wild type at pH 5.5. Therefore, the R29M, E81M, and R29M/E81M mutations appear to negatively impact upon the conformational stability of the CLIC1 intermediate at pH 5.5.

The model selection was further supported by the ANS binding studies that show that no significant binding of ANS was observed along the unfolding curves for wild-type CLIC1 and E81M at pH 7 (Figure 3). However, the R29M and R29M/E81M mutants displayed ANS binding peaks that were not due to protein aggregation at pH 7. The populations of intermediate species observed during urea-induced unfolding at pH 5.5 represented in Figure 4 compare well with the ANS binding observed during urea-induced unfolding at pH 5.5 and 7 (Figure 3).

Effect of the Mutations on the Local Structural Environment. The crystal structures of E81M and R29M/E81M human CLIC1 mutants were determined at 1.84 and 2.0 Å resolution, respectively. The crystallization conditions, X-ray diffraction collection statistics, and refinement statistics are summarized in Table 1. The electron densities for the E81M model and the double mutant model are defined for residues 4-241 and 6-241, respectively. The electron density at position 81 in the E81M model is consistent for methionine, while the electron density at positions 29 and 81 is consistent for methionine in the double mutant. The C^{α} rmsd between the wild-type CLIC1 model (PDB ID: 1K0M) and the mutant models is 0.52 Å (220 residues) and 0.51 Å (219 residues) for E81M and the double mutant, respectively. This indicates that the mutation did not severely alter the backbone structure of the mutants in comparison to the wild-type model. The C^{α} rmsd was calculated using the SPDBV v 4.0 algorithm.[35]

Arg29 and Glu81 are located on α1 and α3, respectively, in the N-domain. These two residues make key H-bond interactions with each other and with some residues, including Asn78, Leu175, and Asn179, within the domain interface (Figure 5a). Four water molecules, within 4 Å distance from Arg29, are involved in mediating some of these H-bond interactions that may contribute to the stability of the N-domain and the domain interface. As shown in Figure 5b, in the wild type, Arg29 makes a salt bridge (ionic) and a H-bond interaction with Glu81, two H-bond interactions with Asn78 (located on α3), and a water-mediated H-bond interaction with Asn179 (located on α6, in the C-domain). Glu81 interacts with

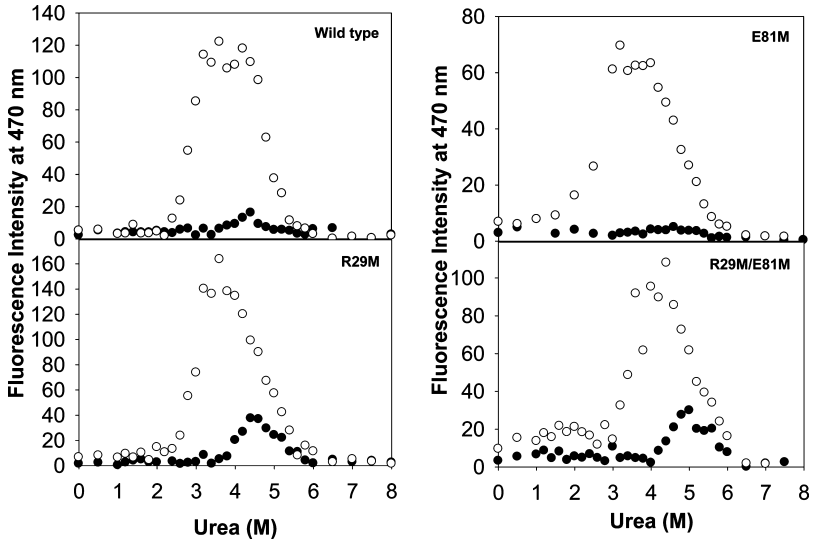

Figure 3. Fluorescence emission at 470 nm of CLIC1 wild type and mutants at pH 7 (●) and pH 5.5 (○) in the presence of ANS. Original spectra were corrected for the fluorescence of the free ANS.

dx.doi.org/10.1021/bi300874b | *Biochemistry* 2012, 51, 7854−7862

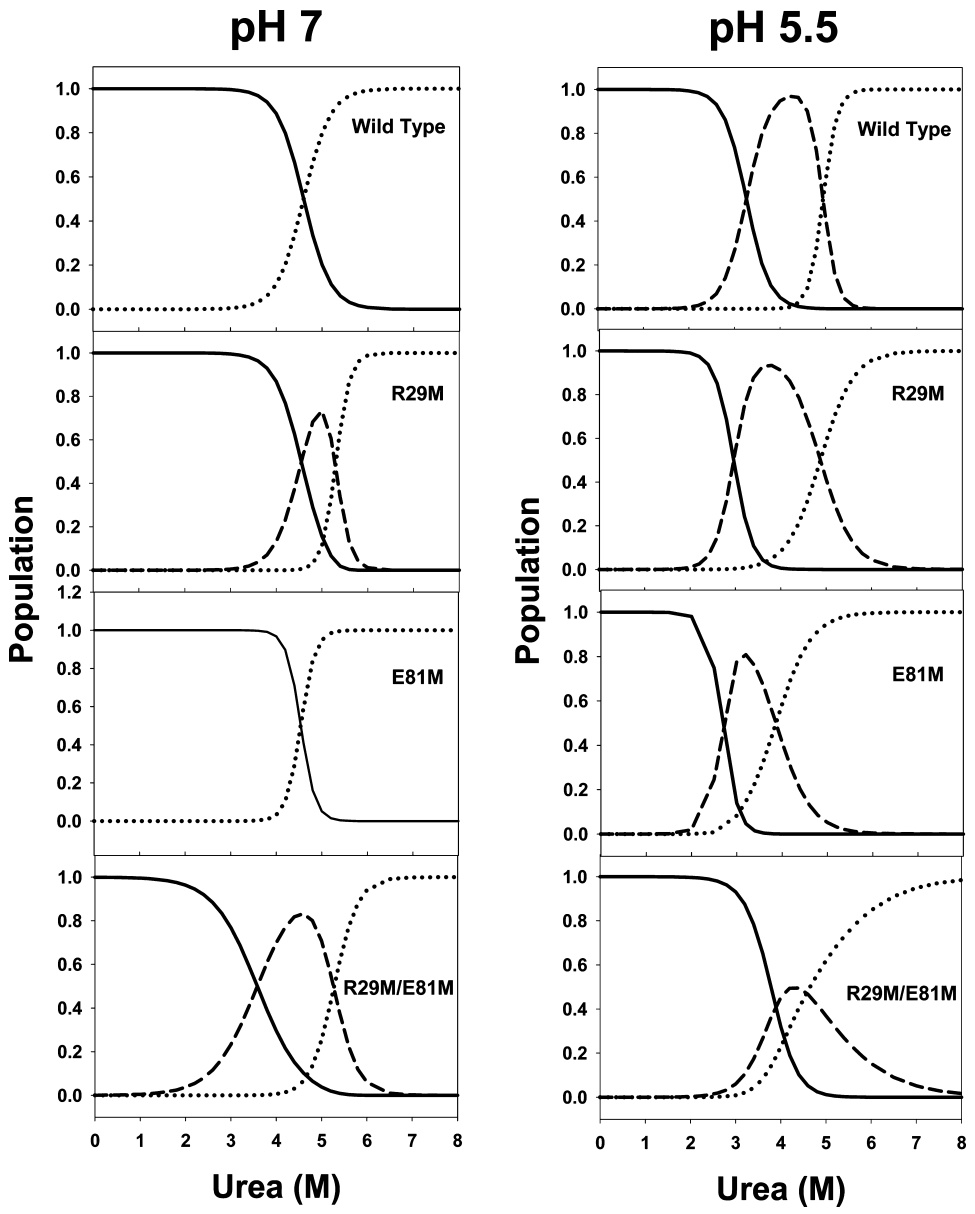

Figure 4. Fractional populations of the native (bold line), unfolded (dots), and intermediate states (dash) as a function of urea concentration. The populations were calculated using the thermodynamic parameters from the global fits to the data for wild type and mutants at pH 7 and pH 5.5.

Leu175 (located on α6) via water-mediated H-bond coordination.

The replacement of Glu81 with the more hydrophobic methionine resulted in a loss of the ionic bond interaction with Arg29 (Figure 5b). However, Arg29 interacts with Met81 via a water-mediated H-bond interaction, with the sulfur atom acting as a H-bond acceptor. Arg29 also maintained a direct H-bond interaction with Asn78 and an indirect water-mediated H-bond interaction with Asn179. Introducing methionine at both positions 29 and 81 resulted in the loss of H-bond interactions between α1, α3, and α6 at the local environment. The hydrophobic side chains of Met29 and Met81 knocked off some of the water molecules that were involved in H-bond interactions that stabilized α1, α3, and α6 the local environment. However, the side-chain orientations of both methionine residues seem to form a van der Waals contact with each other (Figure S5). No cavity was created (using cavity-calculation algorithms implemented in SPDBV v 4.0[35] and PyMOL v 1.3[36]) due to the double mutation. Unfortunately, crystallization of R29M CLIC1 was unsuccessful.

DISCUSSION

The stability of CLIC1 has been demonstrated previously to be pH dependent, and a stable intermediate species has been shown to accumulate under mild denaturing conditions at equilibrium when the pH is dropped from 7 to 5.5.[8] This observation raises the question as to whether certain residues within the structure function as pH-sensitive "switches" that can trigger the changes that are observed when the pH is changed. To address this, we reported in a previous study on the role of the three CLIC1 histidine residues as potential pH-sensitive switches.[38] This study was unable to pinpoint a single residue as being a pH sensor although it did suggest that two of the histidine residues may be involved. The most natural next course of action was to examine the glutamate residues since, depending on their environment, their pK_a could potentially fall

dx.doi.org/10.1021/bi300874b | *Biochemistry* 2012, 51, 7854−7862

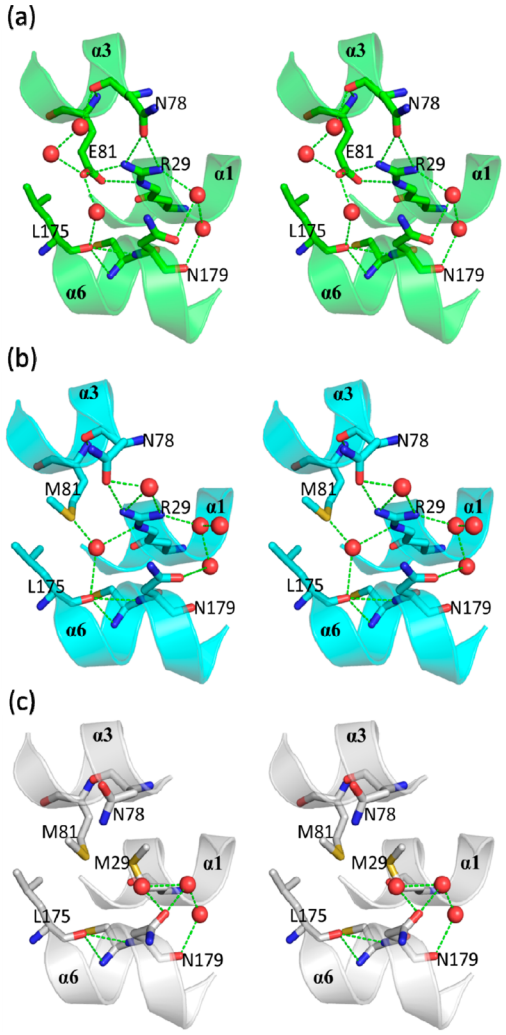

Figure 5. Stereo image illustrating change in H-bond coordination due to the replacement of Glu81 and Arg29 with methionine residue in human CLIC1: (a) wild type, PDB 1K0M; (b) E81M, PDB 3UVH; and (c) R29M/E81M, PDB 3P8W. Spheres represent water molecules forming H-bond interactions within 4 Å vicinity of Arg29 or Glu81 residue. Dashed lines represent an H-bond interaction as computed by SPDBV version 4.0.[35] The images were generated with PyMol.[36]

within the physiological pH range.[20,25] Furthermore, other studies have reported the role of both glutamate and histidine residues as pH sensors.[39−42] Of all the CLIC1 glutamate residues, Glu81 was a most attractive option. Its pK_a in the wild-type protein as predicted by ProPka[20,43] is 5.7, which lies within the range of 7−5.5 where the wild-type stability changes have been observed. Furthermore, and most intriguingly, it forms part of a buried salt bridge with Arg29. Several studies have shown that buried electrostatic interactions in proteins play crucial roles that can affect the structure, function, or conformation of these proteins.[44−50] Arg29 and Glu81 are topologically conserved across the CLIC family (Figure 1a) which points to the significance of this buried interaction. They are both located in the highly dynamic N-domain (Arg29 in helix α1 and Glu81 in helix α3) and are involved in numerous hydrogen-bonding interactions including a salt bridge (Figure 5) that contribute to the stability both in the N-domain and at the domain interface.

In order to establish whether Glu81 functions as a pH sensor and, further, to elucidate the contribution of the conserved Glu81-Arg29 buried salt bridge to CLIC1 stability, we systematically mutated Glu81 and/or Arg29 to methionine which is hydrophobic with a nonionizable side chain. The structural integrity of all the mutants remained intact (Figures S1−S3), and the C^{α} rmsd between the wild-type and mutant structures indicated no major structural changes (Figure 5); hence, changes in stability can be interpreted as arising from the specific effect of the mutation rather than from any global structural alterations.

Wild-type CLIC1 equilibrium unfolding is two-state at pH 7. In this study, we propose that when the pH of the wild type is lowered to 5.5, Glu81 becomes protonated, causing the Glu81-Arg29 salt bridge to break which gives rise to the observed slight destabilization of the native state and the accumulation of a stable intermediate species under mild denaturing conditions (Figure 2 and Table 3). Hence, we created the E81M mutant. Here the negative charge is removed which, in theory, is what should occur in the wild type when the pH is dropped and Glu81 becomes protonated. We would therefore expect E81M CLIC1 at pH 7 to resemble the wild type at pH 5.5 which should be evidenced by the appearance of the equilibrium intermediate at pH 7. We do not see this, however, and unfolding of E81M CLIC1 at equilibrium is two-state at pH 7 as is the wild type (Figure 2). In fact, in a peculiar turn of events, the mutation actually appears to stabilize the protein (Table 3). This can be explained by two observations. First, Met81 forms stabilizing hydrophobic contacts with Val33, Ile80, Leu84, and Leu175. These interactions compensate for the loss of electrostatic contacts normally provided by the charged residue in the wild type.[39] Second, the thermodynamically unfavorable buried positive charge on Arg29 is electrostatically satisfied via a water-mediated hydrogen bond with the Met81 sulfur atom (Figure 5) which mimics the wild-type salt bridge. The combined effect of these events is stabilization of the native state at pH 7. Although the intermediate species is still present at pH 5.5 in the mutant, it has greatly reduced stability (Table 3), and it is significantly less populated (by nearly 2 orders of magnitude) than the wild-type intermediate (Figures 3 and 4) possibly due to the stabilizing influence of Met81 on the native state. Interestingly, though, the total free energy change upon unfolding (ΔG_{nu}) of E81M CLIC1 does not change significantly with pH (Figure S6) so that, although there is an energy shift between the native and intermediate states, the total free energy change is no longer dependent on pH as it is in the wild type. This is comparable to results from our previous study on the histidine mutants.[38] This implies that although protonation of Glu81 is not the sole contributor to the formation of the intermediate species, it certainly is involved.

In order to determine which member of the salt bridge contributed most to the stability of CLIC1, we created the R29M mutant. In this case, breaking the salt bridge by removal of the positive charge resulted in what was expected for the E81M mutant, i.e., destabilization of the native state and detection of an ANS-binding intermediate species at pH 7 (Figures 2, 3, and 4). This indicates that removal of the salt bridge does indeed stabilize the intermediate state. Unfortunately, crystallization of the R29M mutant was unsuccessful so we are only able to speculate that, unlike in the case of the E81M mutation where the loss of the salt bridge is compensated for by a water-mediated hydrogen bond, in the case of R29M, the negatively charged Glu81 is left electrostati-

dx.doi.org/10.1021/bi300874b | *Biochemistry* 2012, 51, 7854−7862

cally unsatisfied at pH 7, resulting in the stabilization of the intermediate state over the native state.

The third mutant that we created was the R29M/E81M double mutant. This mutation removes both contributing parties to the buried salt bridge as well as most of the stabilizing hydrogen-bonding interactions (Figure 5). Assuming Glu81 is a pH sensor, pH should no longer affect this mutant, and at pH 7 it should resemble R29M CLIC1 at pH 5.5 where Glu81 will be protonated and hence will have lost its negative charge. Indeed, the trend is similar. Both the double mutant at pH 7 and R29M at pH 5.5 show a decreased stability of the native state relative to the wild type at pH 7 (Table 3), implying the significance of the salt bridge in maintaining the stability of the native state. Furthermore, the stability of the intermediate state is also reduced compared to the wild-type intermediate state in both cases. This implies that the positive charge of Arg29 is necessary to stabilize the intermediate state in the wild type. The dramatic loss of stability of all states of the double mutant compared to the other mutants and the wild type can be explained by the large number of hydrogen-bonding interactions that were broken by the mutation as well as the lack of stabilizing water molecules in the local environment of these residues (Figure 5).

CONCLUSION

CLIC1 is a metamorphic protein that alters its conformation between a soluble and membrane-bound state. The transition between these two conformations is believed to be initiated in the soluble protein by detachment of the N-domain from the C-domain so that the dynamic N-domain can restructure and then insert into the membrane.[1,6,51−53] When the protein is in the cytoplasm at a pH around 7, Glu81 is negatively charged and forms a buried salt bridge with Arg29. This salt bridge and its surrounding interactions contribute to the stabilization of the native state of the protein. When CLIC1 approaches the low pH (~5.5) at the membrane surface, Glu81 loses its charge and the salt bridge breaks. This facilitates the detachment of helix α6 in the C-domain from helix α3 in the N-domain, and it also further destabilizes the N-domain. A partially structured intermediate state is formed and is stabilized by the positive charge on Arg29. Glu81 does not act alone as a pH sensor, however, but functions in combination with other residues such as His185 and His74.[38]

ASSOCIATED CONTENT

Supporting Information

Figures S1−S6 and Table S1. This material is available free of charge via the Internet at http://pubs.acs.org.

AUTHOR INFORMATION

Corresponding Author

*E-mail heinrich.dirr@wits.ac.za; Tel +27 11 7176352; Fax +27 11 717 6351.

Funding

This work was supported by the University of the Witwatersrand, South African National Research Foundation (grants 60810, 65510, and 68898 to H.W.D), and South African Research Chairs Initiative of the Department of Science and Technology and National Research Foundation (grant 64788 to H.W.D). Any opinion, findings and conclusions or recommendations expressed in this material are those of the author(s) and therefore the National Research Foundation and the Department of Science and Technology do not accept any liability with regard thereto. This work was also supported by the Carnegie Foundation, New York.

Notes

The authors declare no competing financial interest.

ABBREVIATIONS

CLIC, chloride intracellular channel; CD, circular dichroism; GST, glutathione transferase; ANS, 8-anilino-1-naphthalenesulfonate.

REFERENCES

(1) Cromer, B. A., Morton, C. J., Board, P. G., and Parker, M. W. (2002) From glutathione transferase to pore in a CLIC. *Eur. Biophys. J. 31*, 356−364.

(2) Harrop, S. J., DeMaere, M. Z., Fairlie, W. D., Reztsova, T., Valenzuela, S. M., Mazzanti, M., Tonini, R., Qiu, M. R., Jankova, L., Warton, K., Bauskin, A. R., Wu, W. M., Pankhurst, S., Campbell, T. J., Breit, S. N., and Curmi, P. M. (2001) Crystal structure of a soluble form of the intracellular chloride ion channel CLIC1 (NCC27) at 1.4-Å resolution. *J. Biol. Chem. 276*, 44993−45000.

(3) Strange, K., Emma, F., and Jackson, P. S. (1996) Cellular and molecular physiology of volume-sensitive anion channels. *Am. J. Physiol. 270*, C711−730.

(4) Littler, D. R., Harrop, S. J., Fairlie, W. D., Brown, L. J., Pankhurst, G. J., Pankhurst, S., DeMaere, M. Z., Campbell, T. J., Bauskin, A. R., Tonini, R., Mazzanti, M., Breit, S. N., and Curmi, P. M. (2004) The intracellular chloride ion channel protein CLIC1 undergoes a redox-controlled structural transition. *J. Biol. Chem. 279*, 9298−9305.

(5) Littler, D. R., Harrop, S. J., Goodchild, S. C., Phang, J. M., Mynott, A. V., Jiang, L., Valenzuela, S. M., Mazzanti, M., Brown, L. J., Breit, S. N., and Curmi, P. M. (2010) The enigma of the CLIC proteins: Ion channels, redox proteins, enzymes, scaffolding proteins? *FEBS Lett. 584*, 2093−2101.

(6) Ashley, R. H. (2003) Challenging accepted ion channel biology: p64 and the CLIC family of putative intracellular anion channel proteins (Review). *Mol. Membr. Biol. 20*, 1−11.

(7) Berryman, M., and Bretscher, A. (2000) Identification of a novel member of the chloride intracellular channel gene family (CLIC5) that associates with the actin cytoskeleton of placental microvilli. *Mol. Biol. Cell 11*, 1509−1521.

(8) Fanucchi, S., Adamson, R. J., and Dirr, H. W. (2008) Formation of an unfolding intermediate state of soluble chloride intracellular channel protein CLIC1 at acidic pH. *Biochemistry 47*, 11674−11681.

(9) Stoychev, S. H., Nathaniel, C., Fanucchi, S., Brock, M., Li, S., Asmus, K., Woods, V. L., Jr., and Dirr, H. W. (2009) Structural dynamics of soluble chloride intracellular channel protein CLIC1 examined by amide hydrogen-deuterium exchange mass spectrometry. *Biochemistry 48*, 8413−8421.

(10) al-Awqati, Q. (1995) Chloride channels of intracellular organelles. *Curr. Opin. Cell Biol. 7*, 504−508.

(11) Jentsch, T. J., and Gunther, W. (1997) Chloride channels: an emerging molecular picture. *Bioessays 19*, 117−126.

(12) Tonini, R., Ferroni, A., Valenzuela, S. M., Warton, K., Campbell, T. J., Breit, S. N., and Mazzanti, M. (2000) Functional characterization of the NCC27 nuclear protein in stable transfected CHO-K1 cells. *FAEBS J. 14*, 1171−1178.

(13) McLaughlin, S. (1989) The electrostatic properties of membranes. *Annu. Rev. Biophys. Biophys. Chem. 18*, 113−136.

(14) van der Goot, F. G., Gonzalez-Manas, J. M., Lakey, J. H., and Pattus, F. (1991) A 'molten-globule' membrane-insertion intermediate of the pore-forming domain of colicin A. *Nature 354*, 408−410.

(15) Gertsman, I., Fu, C. Y., Huang, R., Komives, E. A., and Johnson, J. E. (2010) Critical salt bridges guide capsid assembly, stability, and maturation behavior in bacteriophage HK97. *Mol. Cell. Proteomics 9*, 1752−1763.

(16) Kumar, S., and Nussinov, R. (1999) Salt bridge stability in monomeric proteins. *J. Mol. Biol. 293*, 1241−1255.
(17) Kumar, S., and Nussinov, R. (2001) Fluctuations in ion pairs and their stabilities in proteins. *Proteins 43*, 433−454.
(18) Takano, K., Scholtz, J. M., Sacchettini, J. C., and Pace, C. N. (2003) The contribution of polar group burial to protein stability is strongly context-dependent. *J. Biol. Chem. 278*, 31790−31795.
(19) Takano, K., Tsuchimori, K., Yamagata, Y., and Yutani, K. (2000) Contribution of salt bridges near the surface of a protein to the conformational stability. *Biochemistry 39*, 12375−12381.
(20) Li, H., Robertson, A. D., and Jensen, J. H. (2005) Very fast empirical prediction and rationalization of protein pKa values. *Proteins 61*, 704−721.
(21) Laemmli, U. K. (1970) Cleavage of structural proteins during the assembly of the head of bacteriophage T4. *Nature 227*, 680−685.
(22) Eftink, M. R., and Ghiron, C. A. (1976) Exposure of tryptophanyl residues in proteins. Quantitative determination by fluorescence quenching studies. *Biochemistry 15*, 672−680.
(23) Beechem, J. M. (1992) Global analysis of biochemical and biophysical data. *Methods Enzymol. 210*, 37−54.
(24) Bilsel, O., Zitzewitz, J. A., Bowers, K. E., and Matthews, C. R. (1999) Folding mechanism of the alpha-subunit of tryptophan synthase, an alpha/beta barrel protein: global analysis highlights the interconversion of multiple native, intermediate, and unfolded forms through parallel channels. *Biochemistry 38*, 1018−1029.
(25) Pace, C. N. (1986) Determination and analysis of urea and guanidine hydrochloride denaturation curves. *Methods Enzymol. 131*, 266−280.
(26) Otwinowski, Z., Minor, W., and Carter, C.W., Jr. (1997) Processing of X-ray diffraction data collected in oscillation mode. *Methods Enzymol. 276*, 307−326.
(27) McCoy, A. J. (2007) Solving structures of protein complexes by molecular replacement with Phaser. *Acta Crystallogr., Sect. D: Biol. Crystallogr. 63*, 32−41.
(28) McCoy, A. J., Grosse-Kunstleve, R. W., Adams, P. D., Winn, M. D., Storoni, L. C., and Read, R. J. (2007) Phaser crystallographic software. *J. Appl. Crystallogr. 40*, 658−674.
(29) Collaborative Computational Project (1994) The CCP4 suite: programs for protein crystallography. *Acta Crystallogr., Sect. D: Biol. Crystallogr. 50*, 760−763.
(30) Parbhoo, N., Stoychev, S. H., Fanucchi, S., Achilonu, I., Adamson, R. J., Fernandes, M., Gildenhuys, S., and Dirr, H. W. (2011) A Conserved Interdomain Interaction Is a Determinant of Folding Cooperativity in the GST Fold. *Biochemistry 50*, 7067−7075.
(31) Murshudov, G. N., Vagin, A. A., and Dodson, E. J. (1997) Refinement of macromolecular structures by the maximum-likelihood method. *Acta Crystallogr., Sect. D: Biol. Crystallogr. 53*, 240−255.
(32) Emsley, P., and Cowtan, K. (2004) Coot: model-building tools for molecular graphics. *Acta Crystallogr., Sect. D: Biol. Crystallogr. 60*, 2126−2132.
(33) Laskowski, R. A., Rullmannn, J. A., MacArthur, M. W., Kaptein, R., and Thornton, J. M. (1996) AQUA and PROCHECK-NMR: programs for checking the quality of protein structures solved by NMR. *J. Biomol. NMR 8*, 477−486.
(34) Chen, V. B., Arendall, W. B., III, Headd, J. J., Keedy, D. A., Immormino, R. M., Kapral, G. J., Murray, L. W., Richardson, J. S., and Richardson, D. C. (2010) MolProbity: all-atom structure validation for macromolecular crystallography. *Acta Crystallogr., Sect. D: Biol. Crystallogr. 66*, 12−21.
(35) Guex, N., and Peitsch, M. C. (1997) SWISS-MODEL and the Swiss-PdbViewer: an environment for comparative protein modeling. *Electrophoresis 18*, 2714−2723.
(36) DeLano, W. L. (2002) *The PyMOL Molecular Graphics System*, DeLano Scientific, San Carlos, CA.
(37) Soulages, J. L. (1998) Chemical denaturation: potential impact of undetected intermediates in the free energy of unfolding and m-values obtained from a two-state assumption. *Biophys. J. 75*, 484−492.
(38) Achilonu, I., Fanucchi, S., Cross, M., Fernandes, M., and Dirr, H. W. (2012) Role of individual histidines in the pH-dependent global stability of human chloride intracellular channel 1. *Biochemistry 51*, 995−1004.
(39) Gonzalez, W., Riedelsberger, J., Morales-Navarro, S. E., Caballero, J., Alzate-Morales, J. H., Gonzalez-Nilo, F. D., and Dreyer, I. (2012) The pH sensor of the plant K+-uptake channel KAT1 is built from a sensory cloud rather than from single key amino acids. *Biochem. J. 442*, 57−63.
(40) Landgraf, K. E., Pilling, C., and Falke, J. J. (2008) Molecular mechanism of an oncogenic mutation that alters membrane targeting: Glu17Lys modifies the PIP lipid specificity of the AKT1 PH domain. *Biochemistry 47*, 12260−12269.
(41) Scrimgeour, N. R., Wilson, D. P., and Rychkov, G. Y. (2012) Glu(1) in the Orai1 pore contributes to fast Ca(2)-dependent inactivation and pH dependence of Ca(2) release-activated Ca(2) (CRAC) current. *Biochem. J. 441*, 743−753.
(42) Thompson, A. N., Posson, D. J., Parsa, P. V., and Nimigean, C. M. (2008) Molecular mechanism of pH sensing in KcsA potassium channels. *Proc. Natl. Acad. Sci. U. S. A. 105*, 6900−6905.
(43) Jensen, J. H., Li, H., Robertson, A. D., and Molina, P. A. (2005) Prediction and rationalization of protein pKa values using QM and QM/MM methods. *J. Phys. Chem. A 109*, 6634−6643.
(44) Arbuzova, A., Wang, L., Wang, J., Hangyas-Mihalyne, G., Murray, D., Honig, B., and McLaughlin, S. (2000) Membrane binding of peptides containing both basic and aromatic residues. Experimental studies with peptides corresponding to the scaffolding region of caveolin and the effector region of MARCK. *Biochemistry 39*, 10330−10339.
(45) Hoh, F., Cave, A., Strub, M. P., Baneres, J. L., and Padilla, A. (2009) Removing the invariant salt bridge of parvalbumin increases flexibility in the AB-loop structure. *Acta Crystallogr., Sect. D: Biol. Crystallogr. 65*, 733−743.
(46) Lounnas, V., and Wade, R. C. (1997) Exceptionally stable salt bridges in cytochrome P450cam have functional roles. *Biochemistry 36*, 5402−5417.
(47) McLaughlin, S., and Aderem, A. (1995) The myristoyl-electrostatic switch: a modulator of reversible protein-membrane interactions. *Trends Biochem. Sci. 20*, 272−276.
(48) Sakurai, K., and Goto, Y. (2002) Manipulating monomer-dimer equilibrium of bovine Beta -lactoglobulin by amino acid substitution. *J. Biol. Chem. 277*, 25735−25740.
(49) Seykora, J. T., Myat, M. M., Allen, L. A., Ravetch, J. V., and Aderem, A. (1996) Molecular determinants of the myristoyl-electrostatic switch of MARCKS. *J. Biol. Chem. 271*, 18797−18802.
(50) Yang, A. S., and Honig, B. (1993) On the pH dependence of protein stability. *J. Mol. Biol. 231*, 459−474.
(51) Goodchild, S. C., Howell, M. W., Littler, D. R., Mandyam, R. A., Sale, K. L., Mazzanti, M., Breit, S. N., Curmi, P. M., and Brown, L. J. (2010) Metamorphic response of the CLIC1 chloride intracellular ion channel protein upon membrane interaction. *Biochemistry 49*, 5278−5289.
(52) Tulk, B. M., Kapadia, S., and Edwards, J. C. (2002) CLIC1 inserts from the aqueous phase into phospholipid membranes, where it functions as an anion channel. *Am. J. Physiol. Cell Physiol. 282*, C1103−1112.
(53) Warton, K., Tonini, R., Fairlie, W. D., Matthews, J. M., Valenzuela, S. M., Qiu, M. R., Wu, W. M., Pankhurst, S., Bauskin, A. R., Harrop, S. J., Campbell, T. J., Curmi, P. M., Breit, S. N., and Mazzanti, M. (2002) Recombinant CLIC1 (NCC27) assembles in lipid bilayers via a pH-dependent two-state process to form chloride ion channels with identical characteristics to those observed in Chinese hamster ovary cells expressing CLIC1. *J. Biol. Chem. 277*, 26003−26011.
(54) Poirot, O., Suhre, K., Abergel, C., O'Toole, E., and Notredame, C. (2004) 3DCoffee@igs: a web server for combining sequences and structures into a multiple sequence alignment. *Nucleic Acids Res. 32*, W37−40.